Articles

Evolution of ZnS Nanostructure Morphology under Interfacial Free-Energy Control

Guoqiang Ren,[†] Zhang Lin,[†] Benjamin Gilbert,[‡] Jing Zhang,[†] Feng Huang,*[,†] and Jingkui Liang[§]

Fujian Institute of Research on the Structure of Matter, National Engineering Research Center for Optoelectronic Crystalline Materials, Chinese Academy of Sciences, Fuzhou, Fujian, 350002, People's Republic of China, Earth Sciences Division, Lawrence Berkeley National Laboratory, Berkeley, California 94720, and Institute of Physics and Center for Condensed Matter Physics, Chinese Academy of Sciences, Beijing 100080, People's Republic of China

Received November 20, 2007. Revised Manuscript Received January 8, 2008

Under hydrothermal conditions and extremely high NaOH activity, ZnS forms nanostructures with complex morphologies that are based upon individual or interpenetrating nanosheets. Nanostructure morphology is independent of the size of the ZnS precursor (3 nm, 20 nm, or bulk) but varies systematically with NaOH concentration, producing compact microspheres, open nest- and flowerlike structures, and finally, individual nanosheets. The observations are consistent with a concept of nanostructure morphology controlled by a single parameter—the interfacial free energy of the ZnS (001) face. The synthesis of thermodynamically stable nanostructures open opportunities for new synthetic routes of materials with complex architectures.

Introduction

Size, shape, and crystal structure are crucial factors in determining the chemical, optical, and electrical properties of nanoscale materials.[1,2] One of the most important goals of modern materials chemistry is the development of simple chemical methods for the large-scale synthesis of nanomaterials with full control of size and morphology. One way to achieve this goal is by controlling the rates of nanoparticle nucleation and the rates of growth of different crystal faces, for example, by introducing organic surfactants during synthesis. From a thermodynamic point of view, surfactants can change the surface free energy of different crystal faces, leading to their preferential growth or elimination. Many researchers have discovered that diverse nanoparticle morphologies can be produced in this way.[3–9]

Nanoparticles are generally metastable relative to the equivalent bulk material, and the introduction of surfactants during synthesis is required to arrest the crystal growth via surface adsorption and thus limit particle size and shape. Because of the inherent thermodynamic tendency for growth, a finite size and shape distribution of metastable nanoparticles is inevitable, despite the development of sophisticated controls on growth kinetics.[10–13] A desirable alternative strategy would be to realize an equilibrium system in which a nanophase with a certain size and shape is thermodynamically stable, so that precursors with any other sizes and shapes will transform into this nanophase spontaneously. Recently, we described an experimental system in which a nanoscale ZnS material is thermodynamically favored and can be formed at the expense of bulk ZnS.[14] We showed that this observation is consistent with a theoretical description involving a negative effective interfacial free energy

* Corresponding author. E-mail: fhuang@fjirsm.ac.cn.
[†] Fujian Institute of Research on the Structure of Matter, National Engineering Research Center for Optoelectronic Crystalline Materials, Chinese Academy of Sciences.
[‡] Lawrence Berkeley National Laboratory.
[§] Institute of Physics and Center for Condensed Matter Physics, Chinese Academy of Sciences.

(1) Ding, Z. F.; Quinn, B. M.; Haram, S. K.; Pell, L. E.; Korgel, B. A.; Bard, A. J. *Science* **2002**, *296*, 1293–1297.
(2) Alivisatos, A. P. *Science* **1996**, *271*, 933–937.
(3) Peng, X.; Manna, L.; Yang, W.; Wickham, J.; Scher, E.; Kadavanich, A.; Alivisatos, A. P. *Nature* **2000**, *404*, 59–61.
(4) Zhong, X.; Xie, R.; Sun, L.; Lieberwirth, I.; Knoll, W. *J. Phys. Chem. B* **2006**, *110*, 2–4.
(5) Peng, Z. A.; Peng, X. *J. Am. Chem. Soc.* **2001**, *123*, 1389–1395.
(6) Pacholski, C.; Kornowski, A.; Weller, H. *Angew. Chem., Int. Ed.* **2002**, *41*, 1188–1191.
(7) Manna, L.; Milliron, D. J.; Meisel, A.; Scher, E. C.; Alivasatos, A. P. *Nat. Mater.* **2003**, *2*, 382–385.
(8) Ould-Ely, T.; Prieto-Centurion, D.; Kumar, A.; Guo, W.; Knowles, W. V.; Asokan, S.; Wong, M. S.; Rusakova, I.; Luettge, A.; Whitmire, K. H. *Chem. Mater.* **2006**, *18*, 1821–1829.
(9) Zitoun, D.; Pinn, N.; Frolet, N.; Belin, C. *J. Am. Chem. Soc.* **2005**, *127*, 15034–15035.
(10) Shevchenko, E. V.; Talapin, D. V.; Murray, C. B.; Brien, S. *J. Am. Chem. Soc.* **2006**, *128*, 3620–3637.
(11) Murray, C. B.; Norris, D. J.; Bawendi, M. G. *J. Am. Chem. Soc.* **1993**, *115*, 8706–8715.
(12) Sun, S.; Murray, C. B.; Weller, D.; Folks, L.; Moser, A. *Science* **2000**, *287*, 1989–1992.
(13) Zhang, H.; Banfield, J. F. *J. Mater. Chem.* **1998**, *8*, 2073–2076.
(14) Lin, Z.; Gilbert, B.; Liu, Q. L.; Ren, G. Q.; Huang, F. *J. Am. Chem. Soc.* **2006**, *128*, 6126–6131.

10.1021/cm703308s CCC: $40.75
Published on Web 03/07/2008

(IFE) for one termination surface of the ZnS structure. The conceptual issues associated with this interpretation are discussed in detail in ref 14. Preferential formation of ZnS nanosheets occurs under conditions of very high NaOH concentration, indicating that it is the strong interactions of NaOH that cause a negative effective IFE of the ZnS (001) face. This demonstrates the possibility of large-scale nanomaterial synthesis using thermodynamic control of size and shape by attaining a negative IFE of one or more faces.

ZnS is an important wide band gap II-VI semiconductor (3.6ev), and has been extensively investigated because of their special properties and potential application. It has been investigated for application in electroluminescence,[15] photoluminescence,[16] photocatalysis,[17] etc. Recent studies show ZnS nanomaterials with various morphologies exhibit interesting optical properties, and considerate efforts have been made to synthesize ZnS nanocrystals and to explore their novel properties.[18–20] In this work, we present a systematic investigation of morphology and crystal structure evolution of ZnS nanomaterials synthesized under conditions in which the effective IFE of the ZnS (001) face ranges from approximately zero to negative. We observe the formation of a series of complex nanostructures and show that their morphology can be described by a simple model of a single parameter, the IFE of the (001) face.

Experimental Section

Nanoparticle Synthesis and Transformation. Three nm ZnS nanoparticles were synthesized in water by the dropwise addition of 0.01 M Na_2S to 0.01 M $Zn(NO_3)_2 \cdot 6H_2O$ at room temperature.[14] Twenty nanometer ZnS was purchased from Aldrich. Bulk ZnS was obtained by treating 3 nm nanocrystalline ZnS in 4 M NaOH aqueous solution for a week at 230 °C and 2.8 MPa in hydrothermal autoclaves. ZnS nanomaterials were obtained by treating 3 nm, 20 nm, and bulk ZnS in different NaOH aqueous solutions at 230 °C and 2.8 MPa in hydrothermal autoclaves. The times for sample treatment are prolonged to ensure the attained products present the characteristic nanostructures under the specific ionic situations. After hydrothermal treatment, samples were quenched to room temperature. The solid material was separated by centrifuging and quickly washed with excess water and ethanol to remove the basic solution, without altering the nanosheets. ZnS is poorly soluble in NaOH,[21] and we ensured that ZnS was present in excess in each experiment (0.2 g of ZnS in 15 mL of NaOH solution at different concentrations). Partial dissolution of the solid ZnS formed a saturated solution within 6 days[14] in which the solid ZnS transformed to the complex nanostructures described below. (Supporting Information Figure S1 provides an example showing the shapes and structure of microspheres do not significantly change further after 7 days.)

X-ray Diffraction. A PANalytical X′ Pert PRO diffractometer with Cu Kα radiation (45 kV, 40 mA) was used to identify the crystal structures of initial and treated samples. If the full width at half-maximum (fwhm) intensity of each peak equal to the machine resolution, the sample can be regarded as bulk material.

Scanning Electron Microscopy. SEM analyses were performed using JSM-6700F scanning electron microscopy (SEM) equipped with an Oxford-INCA energy dispersive X-ray (EDX) spectroscopy.

High-Resolution Transmission Electron Microscopy. HRTEM analyses were performed using a JEOL JEM2010 HRTEM. Samples were prepared for HRTEM study by dispersing ZnS powders onto a holey carbon support.

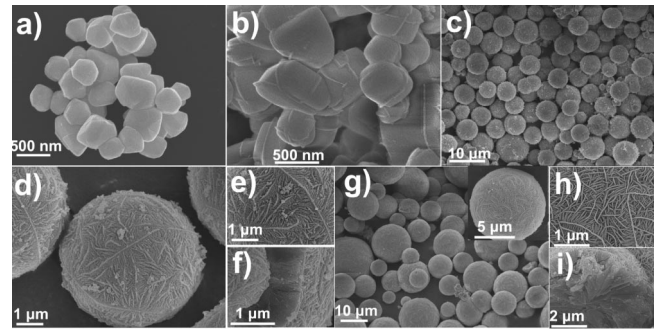

Figure 1. (a) SEM image of the ZnS nanocrystals obtained in different NaOH concentrations at 230 °C and 2.8 MPa in hydrothermal autoclaves: (a) 6 M NaOH, 188 h; (b) 8 M, 188 h; (c) 9 M, 47 days; (d) single microsphere formed at 9 M; (e) high-magnification image of the surface of a microsphere formed at 9 M; (f) high-magnification image of a fractured microsphere formed at 9 M; (g) 10 M, 41 days; insert, single microsphere; (h) high-magnification image of the surface of a microsphere formed at 10 M; (i) fractured microsphere at 10 M.

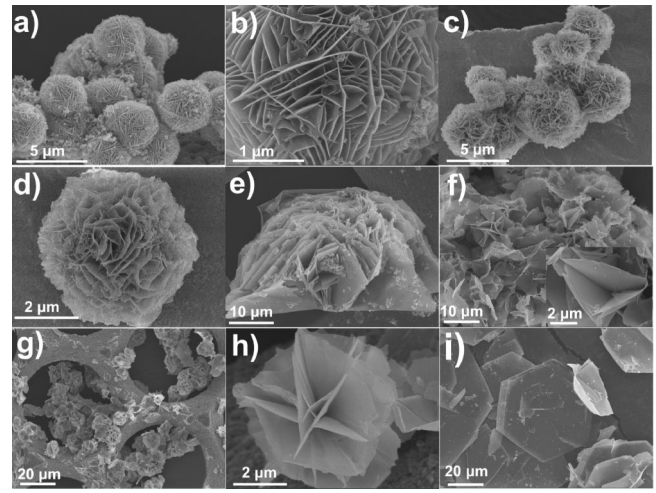

Figure 2. SEM images of ZnS microspheres formed in 11–20 M NaOH: (a) 11 M, 34 days; (b) high-magnification image of microspheres formed at 11 M; (c) 12 M, 30 days; (d) single microsphere formed at 11 M; (e) 14 M, 188 h; (f) 16 M, 36 days; inset, high-magnification image of intersecting nanosheets at the surface of a microsphere formed at 16 M; (g) 17 M, 28 days; (h) single-microsphere formed at 17 M; (i) 20 M, 30 days.

Results

Figures 1 and 2 show SEM images of ZnS nanomaterials produced by hydrothermal treatment of 3 nm ZnS in different concentrations of NaOH. As shown in Figure 1a, the 3 nm ZnS nanoparticles coarsen to form faceted, solid ZnS crystals in 6 M NaOH. With a NaOH concentration of 8 M, the main product is also bulklike ZnS crystals, but some laminar structures are found extending out from the crystal surfaces, indicating the beginning of the growth of nanosheets (Figure

(15) Tang, W.; Cameron, D. C. *Thin Solid Films* **1996**, *280*, 221–226.
(16) Falcony, C.; Garcia, M.; Oritz, A.; Alonso, J. C. *J. Appl. Phys.* **1992**, *72*, 1525–1527.
(17) Fujiwara, H.; Hosokawa, H.; Murakoshi, K.; Wada, Y.; Yanagida, S. *Langmuir* **1998**, *14*, 5154–5159.
(18) Zhu, Y. C.; Bando, Y.; Xue, D. F. *Appl. Phys. Lett.* **2003**, *82*, 1769–1771.
(19) Wang, Z.; Daemen, L.; Zhao, Y.; Zha, C. S.; Down, R. T.; Wang, X.; Wang, Z. L.; Hemley, R. J. *Nat. Mater.* **2005**, *4*, 922–927.
(20) Nanda, J.; Sapra, S.; Sarma, D. D. *Chem. Mater.* **2000**, *12*, 1018–1024.
(21) Laudise, R. A.; Ballman, A. A. *J. Phys. Chem.* **1960**, *64*, 688–691.

1b). At NaOH concentrations of 9 M and above, the initial ZnS material was entirely transformed into complex spherical microstructures (9 M, Figure 1c; 10 M, Figure 1g). High-resolution imaging revealed that each microsphere is composed of numerous ZnS nanosheets that are densely interpenetrated (9 M, images d and e in Figure 1; 10 M, Figure 1h). Atomic force microscope (AFM) observations found the thickness of these nanosheets to be 30–40 nm. Analysis of microspheres that were fractured revealing interior structure showed that the nanosheets extend outward from the center (9 M, Figure 1f; 10 M, Figure 1i). At these concentrations, the diameter of the microspheres ranges from 1 to 10 μm and is controlled by the time of hydrothermal treatment, whereas the thickness of the nanosheet components is constant. The morphology of the ZnS microspheres evolves further when the NaOH concentration is increased to 11 M and above. As shown in Figure 2, there is a clear trend to more open, flowerlike structures at higher NaOH concentration, with consequently less dense nanosheet packing.

A parameter that is suitable to describe the evolution in microsphere morphology is the nanosheet "branching ratio", which we define as the average number of neighboring nanosheets that are incident on given a nanosheet in a microsphere. As shown in Figure 2c−h, the branching ratio of the nanosheets decreases as the NaOH concentration is raised, thus the nanosheet area between branching points increased. At lower branching ratios, the microspheres are significantly less compact and resemble loose nest- or flowerlike structures instead of spheres. In 20 M NaOH, although some nanosheets are interweaved or overlapped, the majority are found as independent flat nanosheets. AFM observation reveals that the thickness of single flat nanosheets formed at 20 M is between 10 and 20 nm.

In summary, we found that NaOH concentration plays a key role in controlling the degree of branching and morphology of the composite microstructures. nanocrystals. The open face areas, the nanosheet thickness and the degree of interweaving are regularly varied depending on the concentration of NaOH.

As shown in Figure 3, X-ray diffraction analysis shows that the ZnS sample produced from 6 M NaOH is a standard sphalerite phase, the *cubic* polytype of ZnS (JCPDS card 77–2100). However, at NaOH concentrations of 8 M and above, a peak at 27.2° appears, which can be indexed as the (100) reflection of wurtzite, the hexagonal polytype.[22] This indicates the existence of hexagonal crystallographic packing in the structure of the nanosheets under conditions of extreme NaOH activity. Simultaneously, the s(111) shows an very noticeable broadening, which can be interpreted as arising from a collapse of the nanostructure occurring on the sphalerite-to-wurtzite phase transformation with increasing NaOH activity.

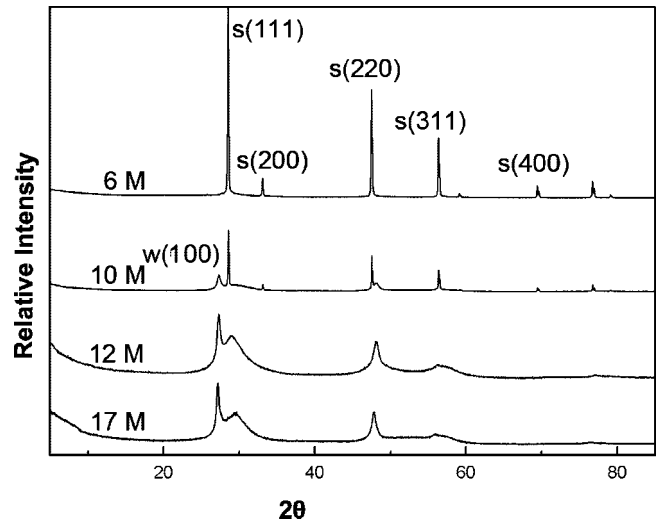

Figure 3. XRD patterns of ZnS nanostructures produced under hydrothermal conditions at different concentrations of NaOH. The samples were quenched to room temperature and thoroughly washed with water before analysis. More details about the structural analysis of water-washed nanosheet can be seen in the Supporting Information, Figure S2.

Figure 4a−c shows transmission electron microscope (TEM) analysis of the ZnS nanocrystals prepared at 12 M NaOH, revealing that the microspheres are composed of nanosheets, consistent with SEM observations. Figure 4b is the HRTEM image and the selected area electron diffraction (SAED) pattern of a piece of nanosheet ultrasonically exfoliated from a microsphere. The SAED pattern shows the individual nanosheet to be a single crystal, with a hexagonal or trigonal symmetry axis perpendicular to the plane of the sheet. Close inspection of the HRTEM image shows that the nanosheet phase exhibits only the hexagonal close-packed ZnS structure, but that it is subdivided into domains of incoherent lattice orientations. Thus, the nanosheets formed in 12 M NaOH are poorly crystalline, as confirmed by Fourier transform (FT) analysis of the HRTEM image (inset to Figure 4c). The orientational disorder leads to the formation of almost complete rings in the reciprocal image.

Figure 4d is a TEM image of ZnS nanosheet prepared at 17 M NaOH. The SAED patterns indicate that the nanosheets are single crystal, and also can be indexed as the [001] zone axis of hexagonal wurtzite-type ZnS crystal (Figure 4e). In contrast to the material formed at 12 M NaOH, HRTEM shows that the structure of the nanosheet is very complete, and no lattice disorder is observed (Figure 4f). Moreover, the FT image of HRTEM of the 17 M sample shows singular reciprocal points that are sharp and clear (inset to Figure 4f).

Spectra g and h in Figure 4 present typical energy-dispersive X-ray (EDX) spectra of the nanomaterials, which reveal the presence of Zn, S, and O, plus Cu from the TEM grid. We attribute the small amount of detected O to surface zinc hydroxyl groups, which are known to form on the surface of ZnS nanoparticles synthesized under basic conditions,[23] as well as NaOH not completely removed by the washing steps.[14] Together with the above results, we deduce

(22) In this work, we have used a large amount of water, instead of ethanol, as the post treatment solvent. We found the water-washed nanosheet does not have the series super-lattice peaks in the [001] direction as the ethanol-washed nanosheet does.[14] The disappearance of the super-lattice structure of nanosheets may caused by the more complete wash of NaOH on the nanosheet surfaces. For more details, please see the Supporting Information.

(23) Gilbert, B.; Huang, F.; Lin, Z.; Goodell, C.; Zhang, H. Z.; Banfield, J. F. *Nano Lett.* **2006**, *6*, 605–610.

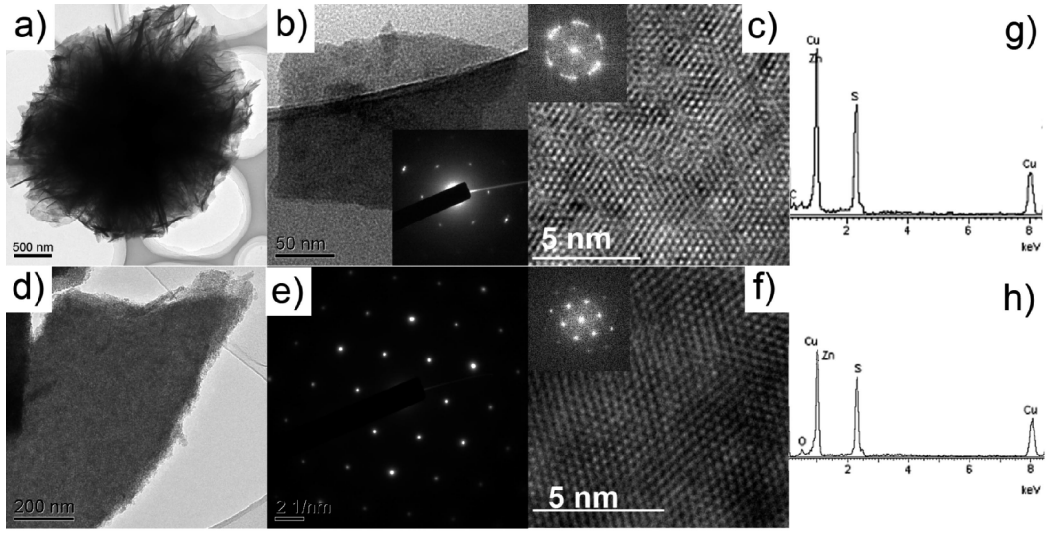

Figure 4. Transmission electron microscope (TEM) images of ZnS microstructures formed at 230 °C in 12 and 17 M NaOH: (a) Low-magnification image of a typical microstructure formed in 12 M NaOH. (b) TEM image of a ZnS nanosheet assembly shed from microstructures; inset, selected area electron diffraction (SAED) pattern acquired from this sample. (c) High-resolution TEM image of an individual ZnS nanosheet; inset, Fourier transform (FT) of the HRTEM image. (d) TEM image of a ZnS nanosheet assembly formed in 17 M NaOH. (e) SAED pattern of sample shown in (d). (f) HRTEM image of an individual ZnS nanosheet; insetn FT of the HRTEM image. (g) Energy-dispersive X-ray (EDX) spectrum from the ZnS material formed in 12 M NaOH. (h) EDX spectrum from the ZnS material formed in 17 M NaOH.

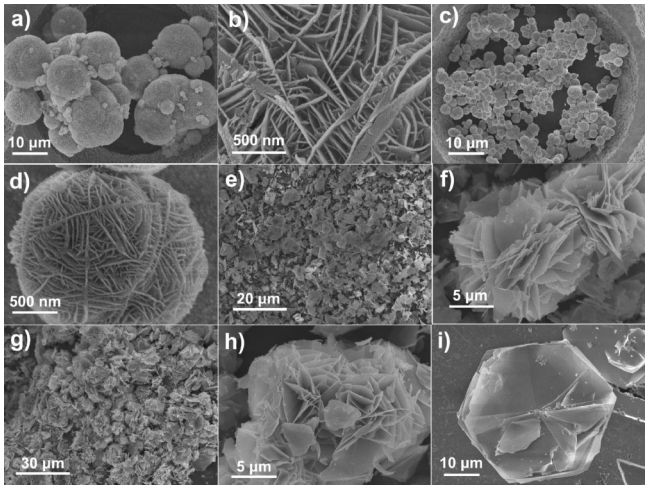

Figure 5. SEM image of the ZnS nanocrystals obtained from ZnS precursor material with different sizes in a range of NaOH concentrations at 230 °C and 2.8 MPa in hydrothermal autoclaves. (a) Bulk ZnS in 10 M NaOH for 30 days. (b) Enlarged image of the sample shown in (a). **c)** 20nm ZnS in 10 M NaOH for 12 h. (d) Enlarged image of the sample shown in (c). (e) Bulk ZnS in 16 M NaOH for 6 days. (f) Enlarged image of the sample shown in (e). (g) 20 nm ZnS in 17 M NaOH for 45 days. (h) Enlarged image of the sample shown in (g). (i) Bulk ZnS in 20 M NaOH for 42 days.

that the nanostructure consists of a ZnS polytype structure. To summarize, highly concentrated NaOH stabilizes a wurtzite type structure of ZnS and the higher the NaOH concentration, the greater the crystallinity of the nanosheet.

In agreement with our previous studies, we found that our results are independent of the size and shape ZnS precursors. As shown by the SEM images in Figure 5, by using 20 nm ZnS and bulk sphalerite ZnS as starting materials, the transformed nanomaterials have the same final morphology and crystal structure as the ZnS nanomaterials produced from 3 nm ZnS at the same NaOH concentration. Hence, ZnS precursors from different sizes (3 nm, 20nm or bulk) can be transformed into structural series in which ZnS nanosheets form microspheres, nestlike, flowerlike, and individual sheets according only to the concentration of NaOH.

Discussion

Relationship of NaOH Concentration and Negative IFE. Previously, we have shown that nanosheets with a hexagonal polytype structure represent the thermodynamically stable phase of ZnS under hydrothermal conditions at 17 M NaOH (see ref 14 and the Supporting Information, Figure S3). Because we obtained nanosheets in which a single crystallographic dimension ([001]) was stabilized in the nanoscale range while the *ab* plane grew without restriction, we concluded that the IFE of the ZnS (001) face was effectively negative under these conditions, whereas the IFE of all other faces remained positive.

In the present experiment, we explored the nanostructures that are formed when the NaOH concentration is varied, and the new results are also consistent with the concept that the NaOH controls the IFE of the (001) face. At relatively low concentrations of NaOH (0–6 M), ZnS precursors of any size will grow directly into bulk crystal, indicating that the IFE of all faces are positive. When the concentration reaches 8 M, ZnS nanosheets begin to grow from the surface of bulk crystal, indicating that the (001) IFE is lowered below zero.

At the critical concentration (8 M NaOH), nano and bulk phases are found to coexist, even after long treatment times. This and other experimental observations may be explained by an illustration of the interfacial contribution to the total free energy of bulk and nanosheet phases, as presented in Figure 6a. Relative to a bulk phase with the same structure, the Gibbs free energy of a nanophase includes an additional interfacial term that is the product of γ, the IFE, and the surface area, A

$$G^{\text{nano}} = G^{\text{bulk}} + \gamma A \qquad (1)$$

A nanoparticle may undergo structural changes in response

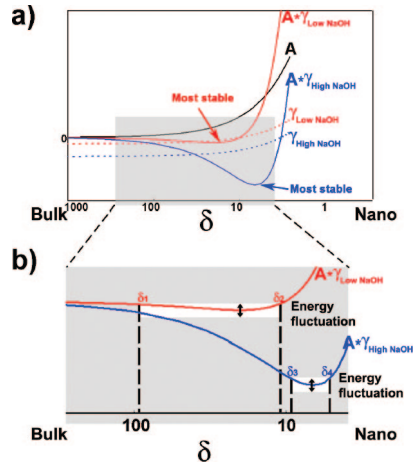

Figure 6. (a) Illustration of the influence of concentration of NaOH on the thermodynamic parameters γ and γA, based on $\gamma = \gamma^{\text{bulk}}{}_0 - (\mu_{\text{ads}} - \mu'_{\text{ads}})\Gamma_{\max} + b/\delta = \gamma^{\text{bulk}} + b/\delta$ developed in ref 14, where δ is the thickness of the nanosheet and b is a constant. It has been shown that γ is dominated by the chemical potential of the adsorbate NaOH, μ_{ads}, and hence the activity of NaOH. Red dashed curve, γ at low concentration of NaOH; blue dash curve, γ at high concentration of NaOH; red solid curve, close to the threshold concentration of NaOH, the total free energy of the nanophase and bulk are approximately equal because γ^{bulk} is negative but close to zero; blue solid curve, at higher NaOH concentrations, for which $\gamma^{\text{bulk}} \ll 0$, the total free energy of the nanophase and bulk are a considerably different. (b) At equilibrium, the range of nanosheet thicknesses obtained is a strong function of the shape of the interfacial free energy function. For a given magnitude of local energy fluctuations, the possible equilibrium thickness values are indicated in white for two different values of γ^{bulk}.

to changes in the surface environment.[23–26] As shown in Figure 6a, when γ is negative but very close to zero, $G^{\text{nano}} \approx G^{\text{bulk}}$, and these phases can coexist. At higher concentrations of NaOH, γ becomes more negative and G^{nano} exhibits a minimum at a certain point between macroscopic and nanoscale dimensions. When γ is sufficiently negative, all bulk ZnS is transformed to the nanophase. Figure 6a shows that the position of the energy minimum varies with γ. This is in agreement with the experimental observation that the nanosheet thickness decreases with increasing NaOH concentration.

Evolution of ZnS Nanostructure Morphology with NaOH Concentration. The thermodynamic description given above predicts that at NaOH concentrations greater than a threshold value all ZnS should be transformed into nanosheets with well-defined thickness. Because the IFE of all surfaces except the (001) face remain positive, the lateral dimensions of the nanosheets should be unrestricted. Our experimental observations revealed more complex behavior. At NaOH concentrations between 9 and 11 M, nanosheets are interleaved together to form microspheres; at concentrations between 12 and 17 M, the degree of interweaving within the microsphere decreased. Only at extremely high NaOH concentrations (>17 M) are individual or stacked nanosheets found. As we discuss later, the observations of these complex structures can be illustrated by a model by

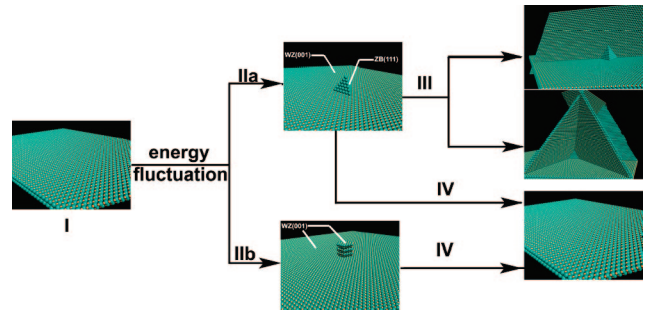

Figure 7. Proposed schematic representation of the growth mechanism of ZnS nanostructures. S atoms are green, Zn atoms are yellow. (I) ZnS nanosheet with wurtzite-type structure. (IIa) Local thickness fluctuation leads to the formation of a hillock with the stacking sequence of sphalerite (zinc blende) structure abcabc. WZ (001) and ZB (111) stand for the isostructural wurtzite (001) and the zinc blende (111) facets, respectively. (IIb) Hillock formation with the stacking sequence of wurtzite abab or related polytype structure. (III) A new nanosheet grows from the ZB structure. (IV) The WZ hillock cannot nucleate a new nanosheet, and the thickness fluctuation dissipates.

considering the statistical fluctuations during the formation of ZnS nanostructures.

The formation of complex microstructures based on interleaved nanosheets may be described by a model in which (001) faces of ZnS nanosheets provide nucleation sites for the growth of new nanosheets. The trend that less compact structures (lower branching ratios) are obtained as NaOH concentration is increased requires that the density of new nucleation sites varies inversely with NaOH concentration. In other words, the surface nucleation density decreases as the (001) IFE becomes more negative. As shown schematically below, these simple assumptions appear sufficient for a good qualitative description for all the observed nanostructures.

One physical mechanism underlying the proposed model could be that new nanosheets are formed from the saturated solution by heterogeneous nucleation, in which the energy barrier for the formation of new nanosheets is reduced for precipitation on existing nanosheet surfaces. However, because increasing NaOH activity decreases the IFE of all ZnS faces, the IFE of spontaneous nuclei would also be lowered, decreasing the barrier for heterogeneous nucleation. This trend would lead to a higher nucleation density and hence more interleaved structures at high NaOH concentration, which is contrary to the observations. Hence, we propose an alternative mechanism: new nanosheets are nucleated by fluctuations in local nanosheet thickness, as depicted in Figure 7. Thermal fluctuations in extrinsic thermodynamic variables are present in all systems at equilibrium, but are proportionally more significant in nanoscale systems.[27,28] Crucially, the (001) face of the wurtzite (WZ) structure is isostructural to the (111) face of the zinc blende (ZB) structure, and the spontaneous formation of ZB hillocks could template up to three new nanosheets (Figure 7; see the Supporting Information, Figure S4). Mixed ZB/W nanostructures ("tetrapods") have previously been demonstrated in CdSe, CdS and PbS.[29–32] WZ structure

(24) Huang, F.; Gilbert, B.; Zhang, H. Z.; Banfield, J. F. *Phys. Rev. Lett.* **2004**, *92*, 155501/1–4.
(25) Zhang, H. Z.; Gilbert, B.; Huang, F.; Banfield, J. F. *Nature* **2003**, *424*, 1025–1028.
(26) Saponjic, Z. V.; Dimitrijevic, N. M.; Tiede, D. M.; Goshe, A. J.; Zuo, X.; Chen, L. Z.; Barnard, A. S.; Zapol, P.; Curtiss, L.; Rajh, T. *Adv. Mater.* **2005**, *17*, 965–971.
(27) Hill, T. L. *Thermodynamics of Small Systems*; Dover Publications: New York, 1994.
(28) Hill, T. L.; Chamberlin, R. V. *Nano Lett.* **2002**, *2*, 609–613.
(29) Manna, L.; Scher, E. C.; Alivisatos, A. P. *J. Am. Chem. Soc.* **2000**, *122*, 12700–12706.

hillocks may initiate growth of existing nanosheet thickness, but cannot nucleate new nanosheets (for more details about this point, please see the Supporting Information, Figure S5). At equilibrium, both WZ and ZB hillocks will form and dissipate, but a fraction of ZB structures will lead to new nanosheet growth. In contrast to a model based on heterogeneous nucleation, the proposed model predicts that new nanosheets are always formed epitaxially, at specific crystallographic orientations relative to the substrate, but this cannot be accurately verified with the imaging data. However, as described below, the present model is in agreement with the trend with NaOH concentration.

Although the magnitude of local energy fluctuations is determined by temperature, the resulting thickness fluctuations are additionally dependent on the shape of the interfacial free energy function depicted in Figure 6b. When IFE is slightly negative, the equilibrium value of nanosheet thickness lies in a shallow energy minimum. Thus, a small energy fluctuation will result in relative large equilibrium range of thickness (from δ_1 to δ_2 in Figure 6b), and a high density of thickness fluctuations is expected, leading to the growth of highly interleaved nanosheets. At higher NaOH concentrations, for which the IFE is more negative, equilibrium nanosheet thickness lies in a deeper minimum, the same magnitude of energy fluctuation will result in a smaller equilibrium range of thickness (from δ_3 to δ_4). Thus nanostructures with lower branching ratios are obtained. The evolution in ZnS nanostructure morphology as a function of interfacial energy is depicted in Figure 8.

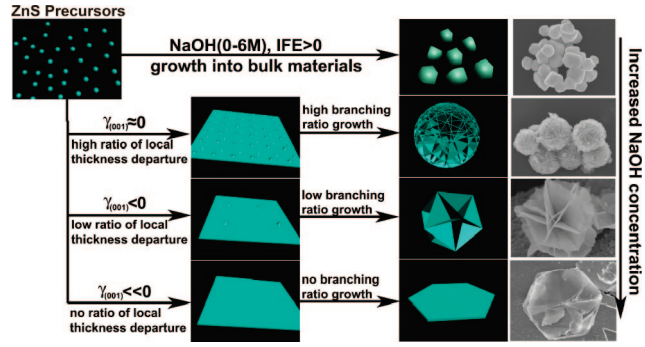

Figure 8. Proposed growth process of nanosheet-based ZnS nanostructures in different NaOH concentrations. The interfacial free energy (IFE) of the wurtzite ZnS (001) face is varied by NaOH concentration, modifying the density of thickness fluctuations that can nucleate the growth of new nanosheets.

Conclusion

In conclusion, we report the evolution of nanosheet-based ZnS nanostructure morphology under conditions of negative IFE. The concentration of NaOH plays the key role in controlling the nanostructure morphology and their branching ratio. The observations are consistent with a model in which statistical fluctuations in nanosheet thickness nucleate the formation of new, interweaved nanosheets with a density that is controlled by the ZnS wurtzite (001) IFE. This work provides an example for controlling the architecture of nanostructure and synthesizing the mass of nanomaterial via the control of negative IFE.

Acknowledgment. We thank Feng Bao, Lihua Zhou, and Chunpeng Yang at Fujian Institute of Research on the Structure of Matter, Chinese Academy of Sciences, for helping with the TEM, SEM, and AFM. Financial support for this study was provided by the Outstanding Youth Fund (50625205), One Hundred Talent Program in Chinese Academy of Sciences, the National Natural Science Foundation of China (Grant 20501021), 973 Program, China (2007CB936703), and the Youth Talent Fund of Fujian Province, China (2007F3113). B.G. acknowledges the support of the Director, Office of Science, U.S. Department of Energy, under Contract DE-AC02-05CH11231.

Supporting Information Available: Time interval investigation of the ZnS microsphere; structure of the nanosheet with different wash treatments; discussion of the face stabilities of ZnS crystal; two-dimensional structural illustration during branch growth (PDF). This material is available free of charge via the Internet at http://pubs.acs.org.

CM703308S

(30) Jun, Y.; Lee, S.; Kang, N.; Cheon, J. *J. Am. Chem. Soc.* **2001**, *123*, 5105–5151.
(31) Lee, S.; Jun, Y.; Cho, S.; Cheon, J. *J. Am. Chem. Soc.* **2002**, *124*, 11244–11245.
(32) When new nanosheets branch grown on the ZB hillocks, they are still restricted in the*c* direction with specific thickness, as pointed out in ref 14 The thickness of the branches can not increase further, whereas the *a* and *b* directions can continue growing. Opposite to what we found, the structure reported in ref 29 was restricted in both the *a* and *b* directions, whereas the *c* direction can continue growing, and thus the tetrapod structure was formed.